Lamellar Thickening in Isotactic Polypropylene with High Tacticity Crystallized at High Temperature

Pralay Maiti,[†] Masamichi Hikosaka,*[,‡] Koji Yamada,[§] Akihiko Toda,[‡] and Fangming Gu[†]

Venture Business Laboratory, Hiroshima University, 2-313 Kagamiyama, Higashi Hiroshima 739-8527, Japan; Faculty of Integrated Arts and Science, Hiroshima University, Higashi Hiroshima 739-8521, Japan; and Oita Research Center, Montell SDK Sunrise Co., Ltd., 2-Nakanosu, Oita 870-0189, Japan

Received April 19, 2000; Revised Manuscript Received September 12, 2000

ABSTRACT: Crystallization behavior of isotactic polypropylene (iPP) with extremely high isotacticity has been studied over a very wide range of crystallization temperature T_c (145 °C ≤ T_c ≤ 166 °C). Optical polarized microscopy observation reveals that morphologies obtained before and after T_c = 157.0 °C are different in nature. Differential scanning calorimetric measurement shows that the melting temperature (T_m) increases significantly with increase of both T_c and crystallization time t. A sudden jump in the slope of T_m versus log t plot is observed at T_c = 157.0 °C, which suggests a kind of order−disorder transition taking place at high T_c (≥157.0 °C) to allow better chain sliding diffusion. Such a disordering has been confirmed by means of X-ray measurements and will be reported in another paper of this series. It was also convinced that annealing at high temperature subsequent to lower temperature crystallization promotes much more rapid lamellar thickening than crystallization alone does at the same high temperature. The lamellar thickness is determined by transmission electron microscopy and also shows a discontinuous upward shift at T_c = 157.0 °C. The lamella with the thickness up to 66 nm is reported for the first time.

1. Introduction

Isotactic polypropylene (iPP) has been well studied over the past four decades because of its uniqueness in the field of polymer crystallization.[1−12] There are several factors affecting the crystallization of iPP such as molecular weight and its distribution, isotacticity, and the crystallization temperature. To get a more ideal structure and morphology of iPP, one needs the sample with narrow molecular weight distribution and high isotacticity.

Lamellar thickening, either via isothermal crystallization or annealing, plays an important role in the final structure and morphology of crystalline polymers. The lamellar thickening rate W is defined by Peterlin[13] as $W = \mathrm{d}l/\mathrm{d}\log t$, where l is lamellar thickness or long period of the stacked lamellae and log t represents the logarithm of crystallization time t. This thickening process, leading to a much more perfect structure, is modeled by Hikosaka[14,15] through chain sliding diffusion theory. Cheng et al.[16] determined the lamellar thickness of fractionated iPP samples by small-angle X-ray scattering (SAXS) and showed that lamellar thickness varies from 8 to 20 nm in the range of the crystallization temperature T_c = 112−152.0 °C.

The morphology of the α form of iPP invokes intense interests due to its unique lamellar crosshatching, which leads to the change in birefringence of the spherulites crystallized at different temperatures.[17−23] Norton and Keller have reviewed and summarized the forms as type I, type II, and mixed spherulites.[21] These classifications are similar to earlier works of Padden and Keith.[22] In particular, the critical analyses of Lotz and his colleagues have clarified that the cause of crosshatching is a unique case of homoepitaxy.[23]

The melting behavior of iPP has become complex in nature not only due to molecular weight and its distribution but also due to different amount of tacticity and the existence of polymorphism (α, β, γ and the mesomorphic form). The interpretation of multiple melting endotherms[11] of iPP has been a matter of controversial debate in the literature. The observed melting behaviors will differ due to a variety of factors including the polymorphism, crosshatching, secondary crystallization and crystal perfection, tacticity, and healing process from thin lamellae to thick ones.

The crystallization behavior of iPP has been well studied in the low T_c region on the samples with lower isotacticity, but only a few studies have been extended into the high T_c region on the samples with high isotacticity.[24,25] As stereoregular defects cannot enter into the lamellae, the incorporation of polypropylene chains into the crystallographic lattice strongly depends on the tacticity of the molecule. Hence, it is expected that one could obtain much more ordered structure and regular morphology when using high isotactic material. The main purpose of the present paper is to examine structure, morphology, and physical properties improvements linked with the use of the iPP with extremely high isotacticity crystallized and annealed in the high-temperature region. Emphasis has been given to find out the noble lamellar thickening with help of better chain sliding diffusion at high temperature (≥157.0 °C) due to the occurrence of "conformational disordering". Actually, a discontinuous jump in the unit cell volume is found at 157 °C, which indicates the occurrence of a first-order phase transition. The details will be reported elsewhere.

[†] Venture Business Laboratory, Hiroshima University.
[‡] Faculty of Integrated Arts and Science, Hiroshima University.
[§] Oita Research Center, Montell SDK Sunrise Co., Ltd.
* To whom correspondence should be addressed.

10.1021/ma000686f CCC: $19.00
Published on Web 10/31/2000

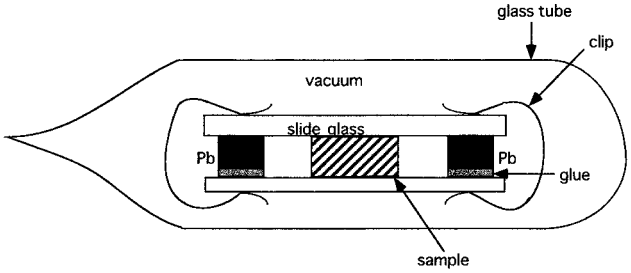

Figure 1. Schematic diagram of sample assembly.

2. Experimental Section

2.1. Materials. The isotactic polypropylene (iPP) supplied by Montell SDK Sunrise Co., Ltd., has molecular weight $M_w = 86.4 \times 10^3$ and $M_w/M_n = 5.6$, as measured by gel permeation chromatography (GPC). The percentage of isotacticity was determined to be 99.5% using ^{13}C high-resolution nuclear magnetic resonance (^{13}C NMR) on the basis of isotactic pentad sequences [mmmm]. It is proper to note here that the iPP, which was synthesized with the $MgCl_2$-supported catalyst, has only meso or racemic sequences and no head-to-head or 1,3-combination. Therefore, the possible stereodefect is only the opposite insertion of monomers.

2.2. Crystallization and Annealing. A small amount of the iPP was first sandwiched between two glass slides. The thickness of the polymer was controlled to be 0.2 mm by inserting metal spacers on both sides of the sample, as shown in Figure 1. To avoid the oxidation, the sample was sealed in a glass tube under vacuum. Since the surface of the sample still might be affected to some extent due to the existence of trace oxygen at high temperature for long hours' heating, the thickness of the sample was kept as large as 0.2 mm. Another advantage of it is the formation of three-dimensional spherulite. The whole glass tube along with the sample was held at 220 °C in an oil bath for 5 min to ensure the complete destroy of any crystalline remnants. After that, they were rapidly transferred to another oil bath that was preset to the desired temperature (145.0−166.0 °C) to allow an isothermal crystallization for various time (from a few hours to 6 months) and then quenched in frozen acetone.

For the annealing experiment, the samples were crystallized first at a lower temperature (T_c = 153.0 °C) for 9 days (full solidification from the melt). Then, they were annealed at a high temperature (T_a = 166.0 °C) for different time.

2.3. Instrumental Studies. After crystallization, the samples were observed using a polarizing optical microscope (POM), Olympus BH-2, fitted with a color-sensitive plate to determine the sign of birefringence.

Thermal analysis was carried out using a modulated DSC, TA Instruments 2920. Either a full spherulite or part of it was cut from the whole crystallized sample and was then heated at a heating rate of 2.0 °C/min purged in a nitrogen atmosphere. The peak temperature in the DSC curve was regarded as the T_m of the crystal. As the enthalpy change was not concerned here, the DSC curves were not normalized. The instrument was calibrated with indium before use.

The lamellar textures of the samples were investigated by a Hitachi H-800 transmission electron microscope (TEM) with the staining technique. A part of spherulite was embedded with the epoxy and then exposed to RuO_4 vapor for 5 h. A thin layer of around 60 nm thick from the stained sample was sectioned at room temperature using the ultra-microtome equipped with a diamond knife. Figure 2 shows the shape of the sample after section. Note the sectional face is parallel to the top surface and around 0.3 mm distance from the center of the spherulite. We would like to emphasize again that the spherulite under investigation is of real three-dimensional species owing to its unusually large thickness (0.2 mm). Such a thickness is much larger than the common one used for POM observation, where the thickness often ranges only a few tens of microns. The resulting iPP films, floating on the water surface, were transferred to copper grids with mesh size 180 by fishing for TEM observation. The thickest lamella was determined by sampling from the TEM micrographs and hence called l_{max} in this study.

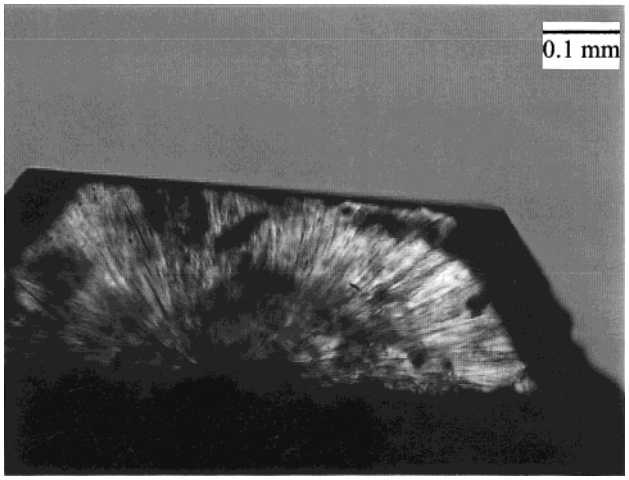

Figure 2. Optical micrograph of the spherulite after section. A thin layer of around 60 nm was sectioned from the top surface and observed by transmission electric microscopy.

3. Results

3.1. Spherulitic Morphology. Figure 3a−f shows optical micrographs of spherulitic morphologies changed with different crystallization temperatures. It is seen that the final spherulitic size (after full solidification) increases with both crystallization time and crystallization temperature. The morphologies formed at low temperature (<157.0 °C, Figure 3a−c) are of spherutic type. Apparently, those formed at high temperature (>157.0 °C, Figure 3d−f) also seem to be spherulitic. However, close observation reveals that the density of the high-temperature morphologies is not uniform and actually reflects some nature of the axialite. Hence, it is fair to conclude that the two sets of morphologies (Figure 3a−c and Figure 3d−f), although very similar in appearance, are different in nature.

3.2. Differential Scanning Calorimetry. Figure 4 and Figure 5 show systematic increase of melting temperature T_m with increase of crystallization temperature T_c and crystallization time t at a particular T_c = 160.0 °C, respectively. Note the thermal analysis was conducted only after full solidification of the melt. It is seen that the change of T_m versus T_c is much more evident than that of T_m versus t at a constant T_c. As a matter of fact, T_m increases linearly with logarithmic crystallization time log t, as shown in Figure 6. It is also to be noted that all the DSC curves of fusion process show single endothermic peaks. On the basis of the above results, it is reasonable to propose that lamellar thickness also increases with increase of both T_c and t. Of special interest is to see that the slope of T_m versus log t line in the high T_c region is steeper than that in the lower temperature region (Figure 6). A sudden jump in the slope values is observed at T_c = 157.0 °C (Figure 7), indicating a faster lamellar thickening rate at high temperature.

The effect of annealing is also shown in Figure 6 by the filled circles with the dashed line. The slope of T_m versus T_a line is much steeper than that of any T_m versus T_c line. The slope of T_m versus T_a line, represented by dashed line, is 4.4. The slope of T_m versus T_c line at T_c = 166.0 °C (2.0) is much steeper than that at T_c = 153.0 °C (0.6).

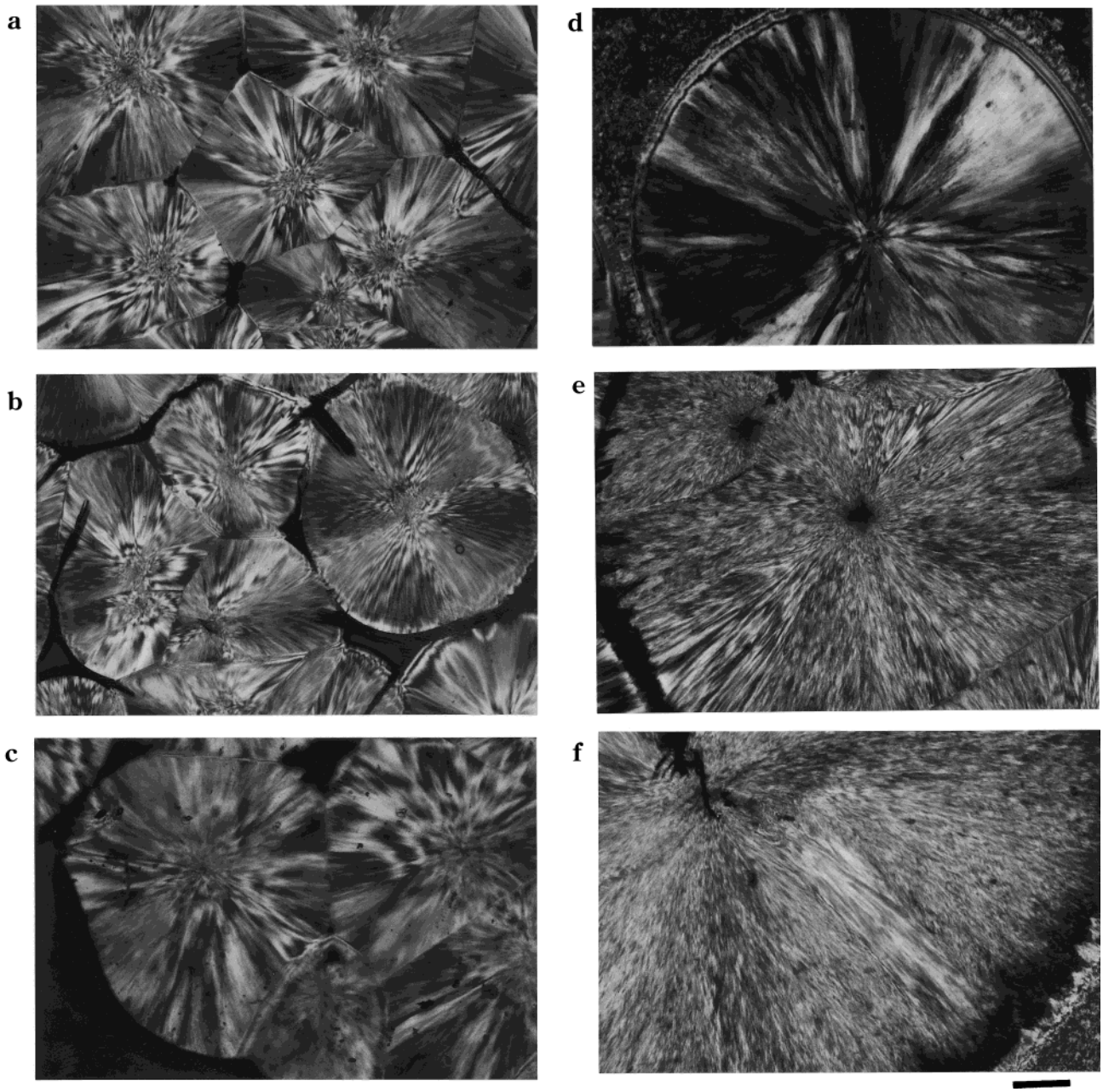

Figure 3. Optical micrographs of the iPP crystallized after full solidification at various temperatures for different times: (a) 145.0 °C for 48 h, (b) 150.0 °C for 101 h, (c) 155.0 °C for 216 h, (d) 157.0 °C for 14 days, (e) 160.0 °C for 28 days, and (f) 166.0 °C for 180 days. The scale bar indicates 0.2 mm.

3.3. Transmission Electron Microscopy (TEM). The variation of lamellar thickness with T_c was confirmed by TEM. Figure 8a−f represents the transmission electron micrographs of the samples crystallized at 145.0, 150.0, 155.0, 157.0, 160.0, and 166.0 °C, respectively. It should be noted here the polymer film under investigation was cut from a real three-dimensional spherulite. Were the crosshatching present in the sample, it should be observed from any specific direction. Since no crosshatching was found in all above TEM micrographs, it was fair to conclude that the crosshatching was absent in the sample. As a matter of fact, it has been revealed in the earlier work that the degree of crosshatching decreases with increase in isotacticity and crystallization temperature. And it will be completely absent in the high-temperature region (≥150 °C) for the iPP with the isotacticity of 99.8%.[25] Admittedly, there should still be some fraction of crosshatched structures existing in the samples crystallized at relatively lower temperatures, say 145.0 and 150.0 °C. On the basis of the earlier work,[25] it can be estimated that the degree of the crosshatching should be less than 5−6% even in the case of T_c = 145.0 °C. Therefore, the crosshatching does not constitute a serious problem here to determine either the average lamellar thickness $\langle l \rangle$ or the maximum lamellar thickness l_{max}. The reason for the latter is more evident since the thickness of the tangential lamella is always thinner than its radial counterpart.

The l_{max}'s were hereby obtained by sampling upon a sufficient number of TEM micrographs for each crystallization temperature. Corresponding to Figure 8a−f, they exhibit the maximum lamellar thickness of 18, 29, 38, 37, 55, and 66 nm at T_c = 145.0, 150.0, 155.0, 157.0, 160.0 and 166.0 °C, respectively. The thickest lamella (66 nm) is reported here for the first time. Figure 9

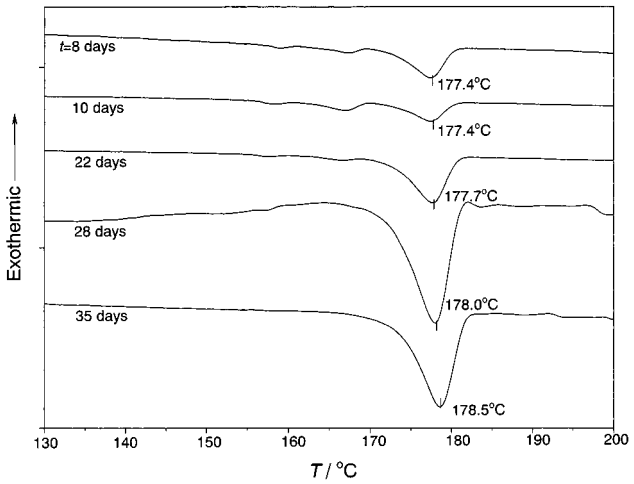

Figure 4. DSC curves of samples crystallized at $T_c = 160.0$ °C for indicated time and then quenched into frozen acetone.

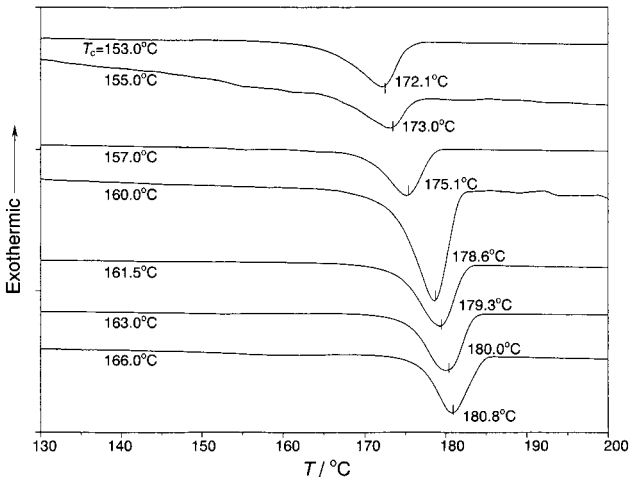

Figure 5. DSC curves of samples crystallized at indicated temperature for sufficient long time to allow a full solidification.

shows the curve of l_{max} as a function of T_c. The actual variations of l_{max} versus T_c can be represented by two discrete lines. A jump in lamellar thickness at $T_c = 157.0$ °C is again observed, which suggests a rapid lamellar thickening rate in the high-temperature region. The reason could be possibly because the diffusion of high isotactic (less defect) molecules within lamellae becomes much easier at high temperature.

4. Discussion

4.1. Effect of T_c and Tacticity on Spherulitic Morphology. It is well-known that spherulite or axialite develops through the initial formation of a frame of dominant lamella. Particularly, embryonic axialites are believed to form through lamellae that are composed of higher percentage of isotactic molecules than the average in the sample.[26] After that, further crystallization, i.e., secondary crystallization or overgrowth, occurs to a degree between the dominant lamellae dictated by the exact composition of the melt. In such a way, subsidiary lamellae occupy the rest space. In fact, Bassett et al.[26] also suggested that the subsidiary lamellae contain shorter molecules on average than do dominant lamellae. It has been confirmed in this study that the initial morphology formed at high temperature is mainly of axialite type. Hence, one may assume that

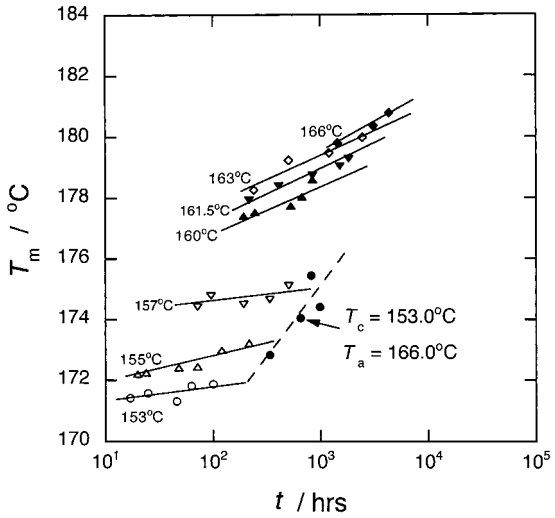

Figure 6. Plot of melting temperature T_m versus logarithmic crystallization time log t.

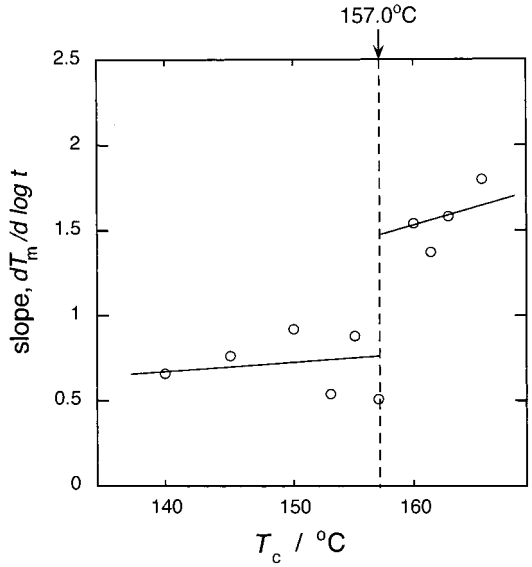

Figure 7. Slope of T_m−log t line versus crystallization temperature T_c.

the overgrowth might be suppressed in the high-temperature region. This tendency becomes much more dominant with increase of tacticity.[25] It is reasonable to suppose that the molecule can be arranged nicely within lamellae with increase of isotacticity. While the molecular chains cannot fit themselves nicely within lamellae with decrease of isotacticity, defects along the chain should be excluded from the lamellae. This becomes origin of the onset of overgrowth, such as stacking of lamellae, branching, and crosshatching, which have been intensively documented in the vast literature.

4.2. Effect of T_c and t on T_m. On the basis of Figures 4 and 5, only one endotherm can be recognized in the DSC curve of fusion process. Using less tactic material, Al-Raheil et al.,[27] however, showed that the double endotherms were often observed in the fusion process. They supposed that the two peaks could be owing to the melting of tangential and radial lamellae, respectively. Using the high isotactic iPP similar to ours, Alamo et al.[24] also demonstrated the well-separated doublet over a wide range of crystallization temperature (135 °C ≤ T_c ≤ 167 °C). On the basis of the observation with

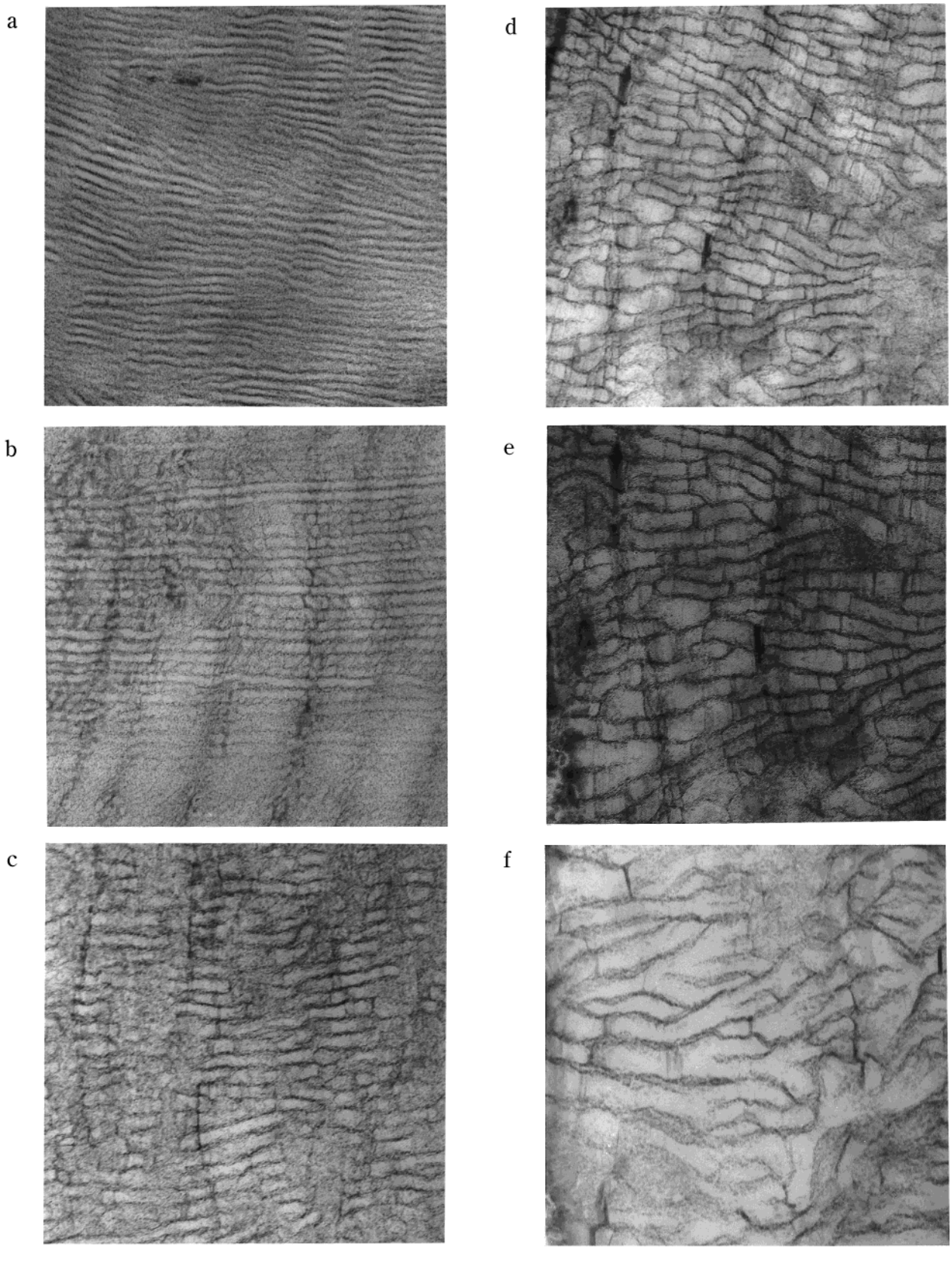

Figure 8. Transmission electron micrographs of iPP samples crystallized at (a) 145.0 °C for 48 h, (b) 150.0 °C for 101 h, (c) 155.0 °C for 216 h, (d) 157.0 °C for 14 days, (e) 160.0 °C for 28 days, and (f) 166.0 °C for 180 days. The scale bar indicates 100 nm.

polarizing optical microscope, they drew the same conclusion as Al-Raheil's. Recently, the above puzzling was solved by Yamada et al.[28] Using well-fractionated iPP with high isotacticity, they confirmed the existence of doublets in the DSC measurements. Only one exceptional case, i.e., the observation of the single melting peak, was observed for the sample having relatively low molecular weight ($M_n = 24 \times 10^3$, $M_w/M_n = 2.2$). They

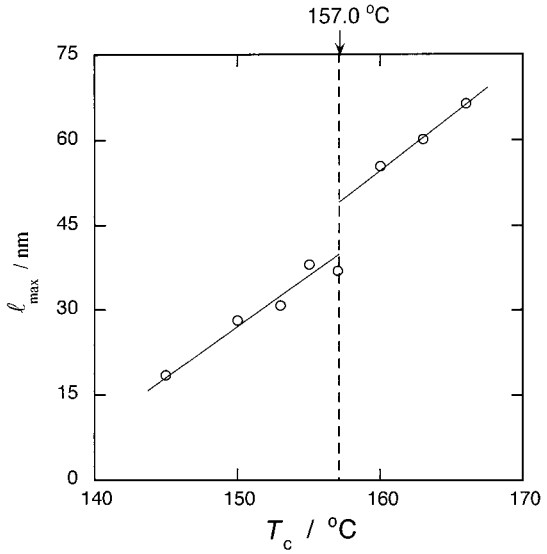

Figure 9. Plot of the maximum lamellar thickness l_{max} versus crystallization temperature T_c.

emphasized that such an observation does not necessarily mean the existence of crosshatching. By means of the TEM observation, they have already shown that the crosshatching was completely absent for the high isotactic sample melt-crystallized at high temperature.[25] Alternatively, they argued that two sets of lamellae with quite different thickness should exist in their sample.

In our case, the situation becomes even more complicated due to the wide distribution of the molecular weight. Furthermore, it was generally accepted that the tacticity strongly differs from the change in the molecular weight. The sample with low molecular weight has a lower isotacticity, and the sample with large molecular weight has a much higher isotacticity. Any DSC curve in Figures 4 and 5 shows a single endotherm having a wide profile (10 °C interval). Therefore, we would conclude that the DSC curve should be a convoluted one constituting many components.

One also can recognize a very small but broad endotherm at lower temperature in the DSC scans of the samples that were crystallized for a relatively short time (8 and 10 days in Figure 4). This small peak can be assigned to the melting of quenched part, which had not been fully solidified yet within that time period.

As shown in Figure 7, the slopes of T_m−log t lines ($dT_m/d \log t$) in the lower- and high-temperature regions are 0.7 and 1.6, respectively. The sudden jump in the slope value (Figure 7) at $T_c = 157.0$ °C suggests there exists a kind of disordering, which allows a faster lamellar thickening at high temperature through chain sliding diffusion.[14,15] Furthermore, the significant lamellar thickening is also revealed in the annealing experiments, where a much steeper slope of T_m versus T_a line than that of any T_m versus T_c line is observed. Hence, a faster lamellar thickening is again confirmed at high temperature.

4.3. Lamellar Thickening Due to Conformational Disordering at High T_c. Naturally, one may ask what kind of disordering takes place at 157.0 °C and why it could be related to the drastic increase in the slope of T_m−log t curve and the lamellar thickening rate. To answer such a question, some additional X-ray measurements were conducted on the sample that was annealed at different temperatures. It was found that the lattice constants a and b experience a sudden increase, while the c shrinks and the β does not change at $T_a = 157$ °C. When the sample was brought back to room temperature, all lattice constants recovered their original values. It is thus easy to show that the unit cell volume also experiences a discontinuous 0.3% increase at the aforementioned temperature. According to the well-known Clausius−Clapeyron equation, $\Delta S = (dp/dT)\Delta V$, if the observed change in the unit cell volume $\Delta V \neq 0$, it was immediately apparent to obtain $\Delta S \neq 0$, which means $(\partial G/\partial T)_{p,\alpha 2} \neq (\partial G/\partial T)_{p,\alpha 3}$. It is the basic definition in the thermodynamics that when the first derivative of Gibbs free energy (G), $(\partial G/\partial T)_p = -S$, shows discontinuity at $T_{\alpha 2-\alpha 3}$, the first-order phase transition occurs.[29] Note the structure in the new phase was termed to be the "α3" form. We would like to put special emphasis on the concept that the first-order phase transition does not necessarily require any change in symmetry and chain conformation. Such a phase transition can also be regarded as a kind of conformational disordering occurred at high temperature. A more complete description will be reported later.[30]

To sum up, the molecular chains would become much more mobile, hereby promoting better chain sliding diffusion after the occurrence of conformational disordering at 157 °C. For this reason, it is hardly surprising to observe the drastic increases in the slope of T_m−log t curve and lamellar thickening rate at $T \geq 157.0$ °C, as clearly shown in the present study.

5. Conclusion

1. Differential scanning calorimetric measurement shows that the melting temperature (T_m) of iPP increases significantly with increase of both T_c and crystallization time t.

2. A sudden jump from 0.7 to 1.6 of the ($dT_m/d \log t$) value at $T_c = 157.0$ °C is observed, indicating a much faster lamellar thickening rate above 157.0 °C. Annealing at high temperature subsequent to lower temperature crystallization shows a faster lamellar thickening rate than crystallization alone does at the same high temperature.

3. The lamellar thickness was determined by TEM. The discontinuous upward shift in l_{max} versus T_c line is observed again at $T_c = 157.0$ °C. When the sample was crystallized at $T_c = 166.0$ °C for 6 months, the thickest lamella of 66 nm ever reported is found.

4. Sudden jumps in the slope of T_m versus log t line and l_{max} versus T_c line at 157.0 °C suggest the occurrence of a kind of disordering, which has been confirmed by X-ray diffraction experiments and will be reported in another paper of this series.

Acknowledgment. The authors acknowledge the financial support from the Grant-in Aid for Scientific Research on Priority Areas B2 No. 12127205 and Scientific Research A2 No. 12305062. Our additional thanks are due to Dr. B. Lotz for his valuable advice in the revision of this paper.

References and Notes

(1) Lovinger, A. J.; Chua, J. D.; Gryte, L. C. *J. Polym. Sci., Polym. Phys. Ed.* **1977**, *15*, 641.
(2) Padden, F. J., Jr.; Keith, H. D. *J. Appl. Phys.* **1959**, *30*, 1479.
(3) Cheng, S. Z. D.; Janimak, J. J.; Zhang, A.-Q.; Cheng, H. N. *Macromolecules* **1990**, *23*, 298.
(4) Clark, E. J.; Hoffman, J. D. *Macromolecules* **1984**, *17*, 878.
(5) Goldfarb, L. *Makromol. Chem.* **1978**, *179*, 2297.

(6) Campbell, R. A.; Phillips, P. J. *Bull. Am. Phys. Soc.* **1988**, *33*, 546; **1989**, *34*, 754.
(7) Binsbergen, F. L.; DeLange, B. G. M. *Polymer* **1968**, *9*, 23.
(8) Martuscelli, E.; Silvestre, C.; Abate, G. *Polymer* **1982**, *23*, 229.
(9) Allen, R. C.; Mandelkern, L. *Polym. Bull.* **1987**, *17*, 473.
(10) Wlochowicz, A.; Eder, M. *Polymer* **1981**, *22*, 1285.
(11) Janimak, J. J.; Cheng, S. Z. D.; Zhang, A.; Hsieh, E. T. *Polymer* **1992**, *33*, 728.
(12) Guerra, G.; Petraccone; V.; Corradini, P.; De Rosa, C.; Napolitano, R.; Pirozzi, B.; Giunchi, G. *J. Polym. Sci., Polym. Phys. Ed.* **1984**, *22*, 1029.
(13) Peterlin, A. *Macromol. Chem.* **1964**, *74*, 107.
(14) Hikosaka, M. *Polymer* **1987**, *28*, 1257.
(15) Hikosaka, M. *Polymer* **1990**, *31*, 458.
(16) Cheng, S. Z. D.; Janimak, J. J.; Zhang, A.-Q.; Hsieh, E. T. *Polymer* **1991**, *32*, 648.
(17) Bassett, D. C.; Olley, R. H. *Polymer* **1984**, *25*, 935.
(18) Khoury, F. *J. Res. Natl. Bur. Stand. (A)* **1966**, *70*, 29.
(19) Lovinger, A. J. *J. Polym Sci., Polym. Phys. Ed.* **1983**, *21*, 97.
(20) Morrow, D. R.; Newman, B. A. *J. Appl. Phys.* **1986**, *39*, 4944.
(21) Norton, D. R.; Keller, A. *Polymer* **1985**, *26*, 704.
(22) Padden, F. J., Jr.; Keith, H. D. *J. Appl. Phys.* **1966**, *37*, 4013.
(23) Lotz, B.; Wittman, J. C. *J. Polym. Sci., Polym. Phys. Ed.* **1986**, *24*, 1541.
(24) Alamo, R. G.; Brown, G. M.; Mandelkern, L.; Lehtinen, A.; Paukkeri, R. *Polymer* **1999**, *40*, 3933.
(25) Yamada, K.; Matsumoto, S.; Tagashira, K.; Hikosaka, M. *Polymer* **1998**, *39*, 5327.
(26) Bassett, D. C.; Vaughan, A. S. *Polymer* **1985**, *26*, 717.
(27) Al-Raheil, I. A.; Qudah, A. M.; Al-Share, M. *J. Appl. Polym. Sci.* **1998**, *67*, 1267.
(28) Yamada, K., private communication.
(29) Laidler, K. J.; Meiser, J. H. *Physical Chemistry*; Houghton Mifflin Co.: Boston, 1999.
(30) Gu, F.; Hikosaka, M.; Zhang, J.; Toda, A., submitted to *Macromolecules*.

MA000686F